

## CHAPTER 3

### MEASURING METHODS AND RESULTS

#### 3.1 Time-integrated measurements of indoor radon concentrations using unfiltered track detectors.

Indoor radon was determined by measuring the  $\alpha$ -decay rate of radon with an unfiltered Kodak LR-115 type II track detector. An unfiltered track detector is a piece of cellulose nitrate film. Alpha particles emitted by radon and its decay products in air strike the detector and produce submicroscopic damage tracks. Cellulose nitrate is sensitive to alpha energies between 1.5 Mev and 4.8 Mev. It is not sensitive to radon decay products that plate out on the detector since their energies are above 5 Mev.

For this study, a small rectangular piece of unfiltered track detector 1 centimeter by 2 centimeters was attached to a rectangular cardboard/aluminum foil socket 4 centimeters by 5 centimeters and had a 1 centimeters by 1 centimeters hole cut in its middle. The cellulose nitrate film was attached to this hole by embedding 0.5 centimeter of its length on both sides of the hole. This left 1 square centimeter of the cellulose nitrate film exposed in the hole. Figure 3.1 shows how the detector was prepared.

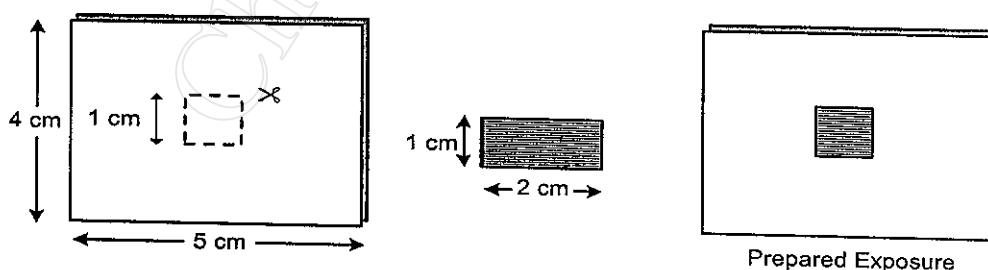


Figure 3.1 Unfiltered track preparation.

After exposure, all detectors were chemically etched in 10 percent sodium hydroxide solution at 60° Celsius for 90 minutes. The equipment used to etch the detectors is show in Figure 3.2.

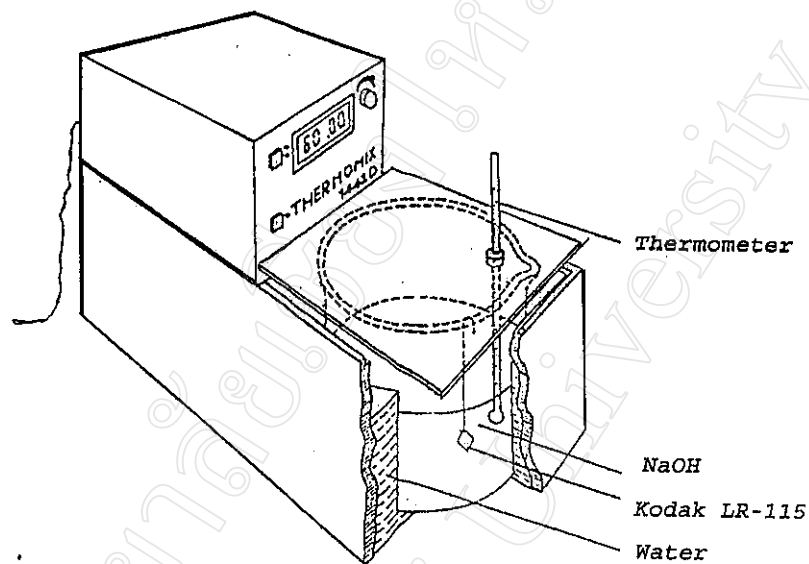


Figure 3.2 Equipment used to etch detector.

After etching, the enlarged alpha tracks (Figure 3.3) were counted on a computer monitor after having been transferred to the computer from a 50-power optical microscope through a video camera, as shown in Figure 3.4.

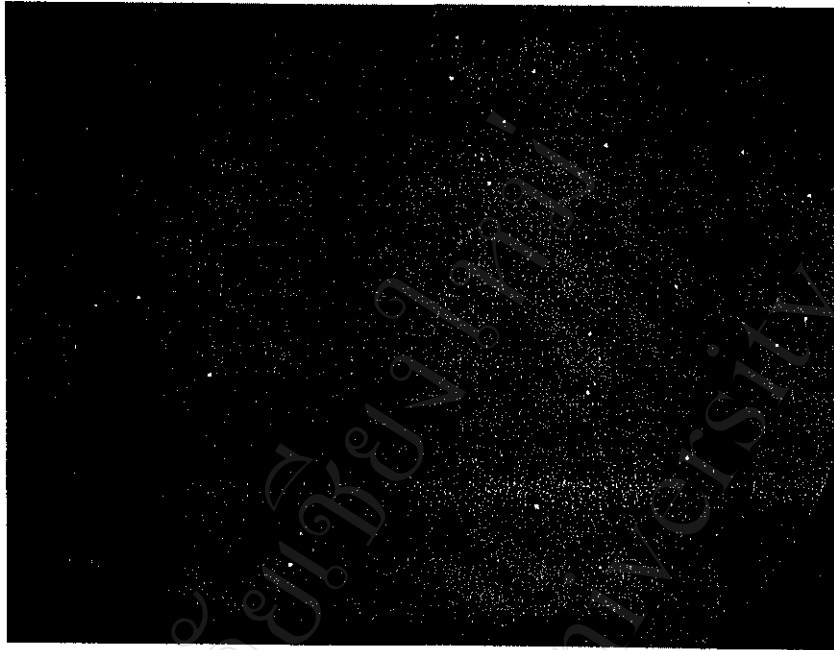


Figure 3.3 PC monitor view of a 4-square millimeter cellulose nitrate detector.

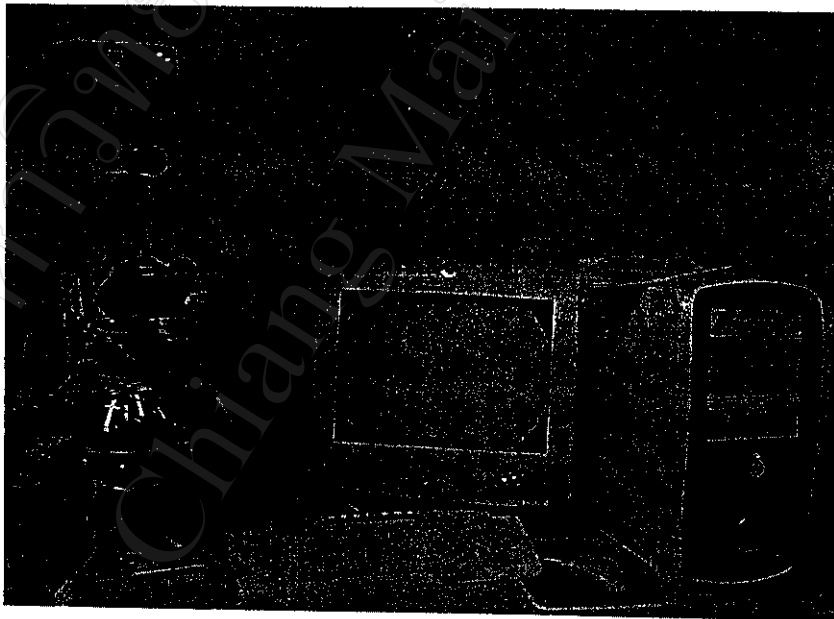


Figure 3.4 Equipment used for enlarging cellulose nitrate detector film.

The net track density was obtained by counting tracks on the exposed area of the detector and then deducting background tracks. The conversion factor used to convert track densities to radon concentrations was  $4 \text{ track.cm}^{-2}/\text{kBq.h.m}^{-3}$  (as the sensitivity of the cellulose nitrate film). This conversion of track densities to radon concentrations followed the experiments of Hertzman and Samuelsson (1986) and Cherouati and others (1988).

In this study, indoor radon measurements were made in 40 houses during three seasons, starting in the rainy season. The first measurements were made from 12 September to 19 October 2001, the next measurements were in the winter from 10 January to 10 March 2002, and the last were made in the summer from 12 April to 11 June 2002. The annual average indoor radon concentration of each house became the mean value for the three seasons. The results of these measurements of indoor radon concentrations from the 40 houses are shown in Figure 3.5.

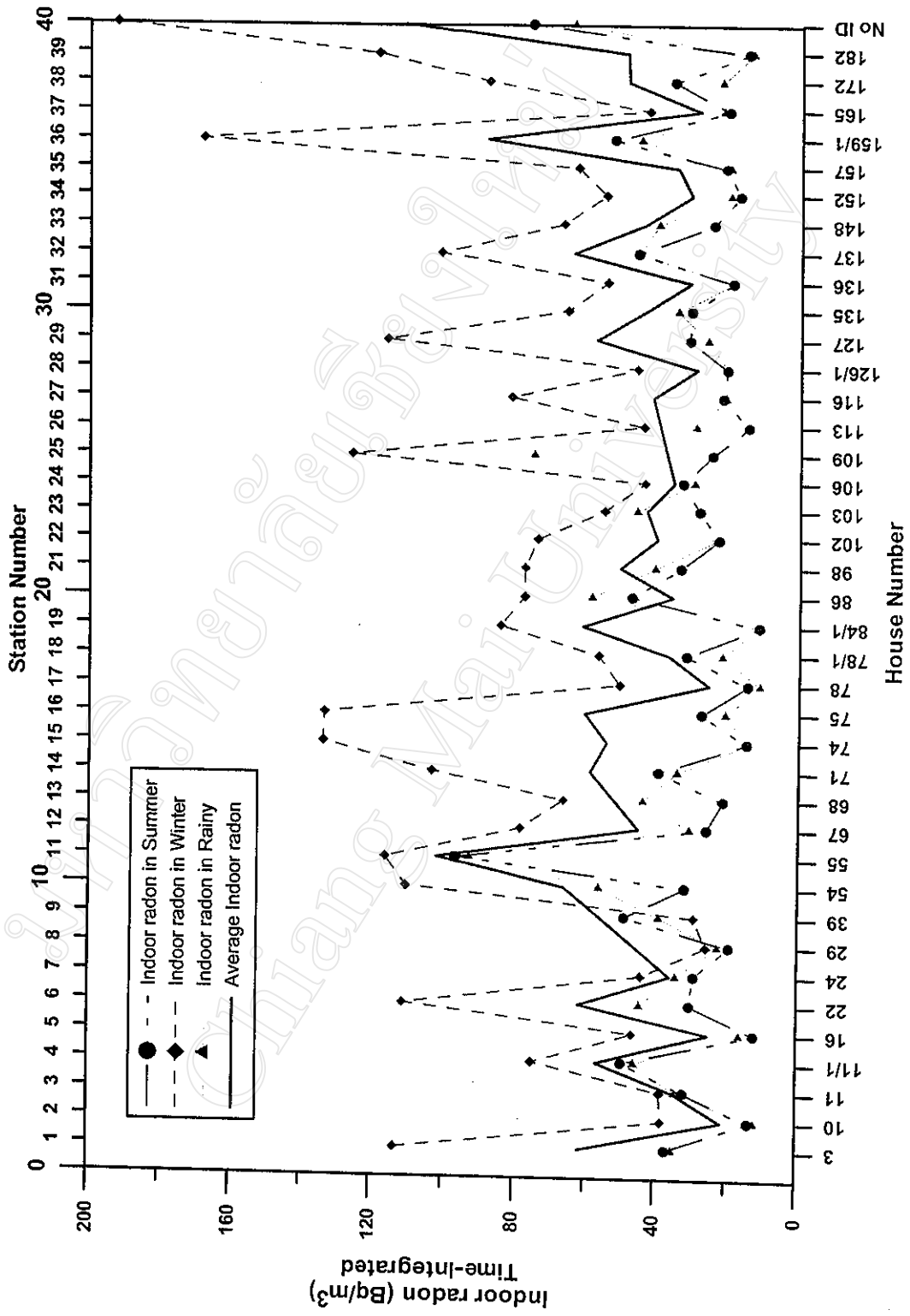


Figure 3.5 Time-integrated indoor radon concentrations from 40 houses during three seasons

### **3.2 Grab sampling measurements of indoor and soil-gas radon concentrations.**

In order to monitor the short-term variation of indoor radon, a grab sampling method was used for indoor radon measurements at a base house. The measurements were made during winter, from 28 January to 3 March 2002, and summer, from 21 May to 30 May 2002. The equipment used for these measurements was a Scintrex RDA-200 radon meter, a filter and filter holder assembly, scintillation cells, and an air pump that could deliver 2 to 10 liters of air per minute. The Scintrex radon meter electronics console is designed to measure the alpha particle activity originating from radon and its daughters. The alpha particles register on the zinc sulphide phosphor coating of the scintillation cell or tray in the form of light flashes. The intrinsic scintillation properties of the phosphor are highly sensitive to alpha particles in the 5.5 Mev energy range that result from the decay of isotopic radon in its gas phase. Each flash of light seen by the high gain photomultiplier tube is transformed into an electrical impulse. These electrical impulses are then recorded by the scaler circuitry to provide a cumulative count and to display this count digitally, after completing a preset counting sequence. Therefore, what is registered on the display is proportional to the alpha particles activating the photomultiplier tube (RDA-200 Operation Manual, 1994).

Short-term variation of indoor radon is start by inserting a fresh scintillation cell into the counting system and then leaving the system to adapt to the dark for 2 to 3 minutes. This ensures that no accidental light exposure contributes to the counting. Background count data need to be determined before injecting indoor gas into the scintillation cell. This is done by counting the background flashes for 5 minutes and stating this number in counts per minute. Indoor air passed through the filter, where the radon progeny is removed. This filtered air is injected twenty liters into the scintillation cell by air pump, the time is noted, and the time of pumping is calculated from the flow rate. The filter holder assembly and

the air pump are then disconnected. Figure 3.6 is a diagram of the process involved.

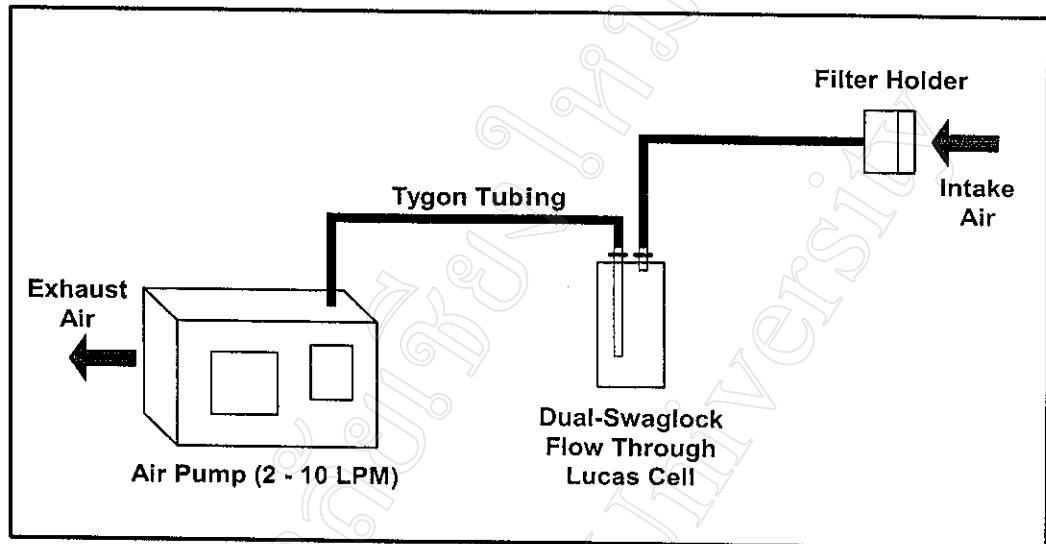


Figure 3.6 Schematic diagram for measuring an indoor radon grab sample

After injection, the cell is set aside and left to decay for 3 hours and 40 minutes. This allows for the equilibrium between radon and its progeny within the cell. The cell is then placed into the counting system for counting and is allowed to adapt to the dark again, count the cell sample for 60 minutes and record in count per minutes (RDA-200 Operation Manual, 1994).

A conversion factor used to convert indoor radon in counts per minute to indoor radon concentration in  $\text{pCi.L}^{-1}$  and/or  $\text{Bq.m}^{-3}$  was the efficiency value of each scintillation cell that was calibrated from the Office of Atomic Energy for Peace in Bangkok (Appendix B).

The short-term variation of indoor radon concentration is shown in Figures 3.7 and 3.8.

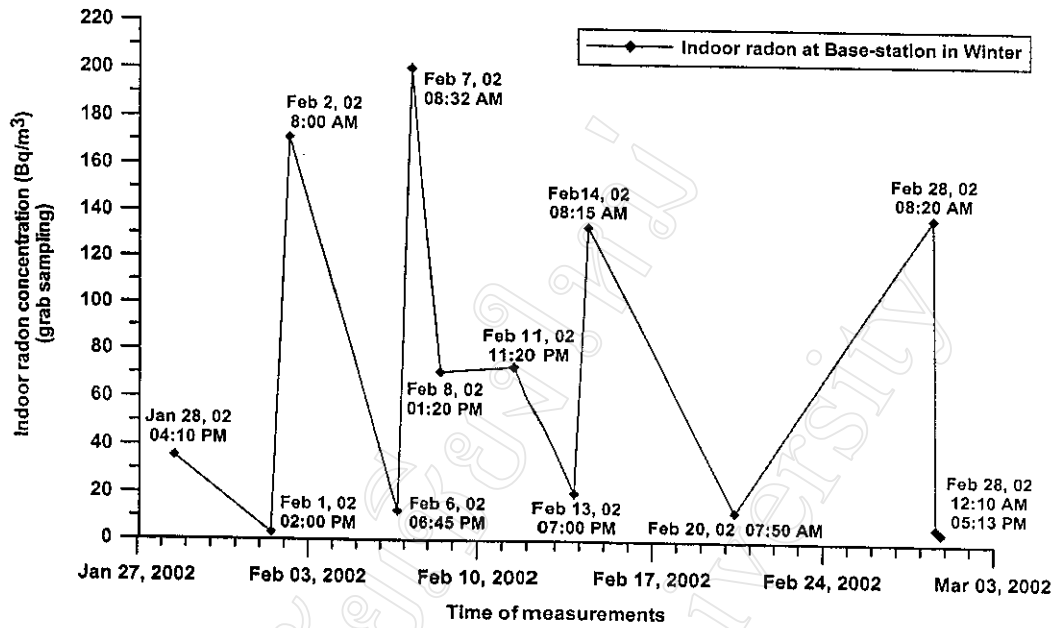


Figure 3.7 Winter indoor radon concentration in the base house.

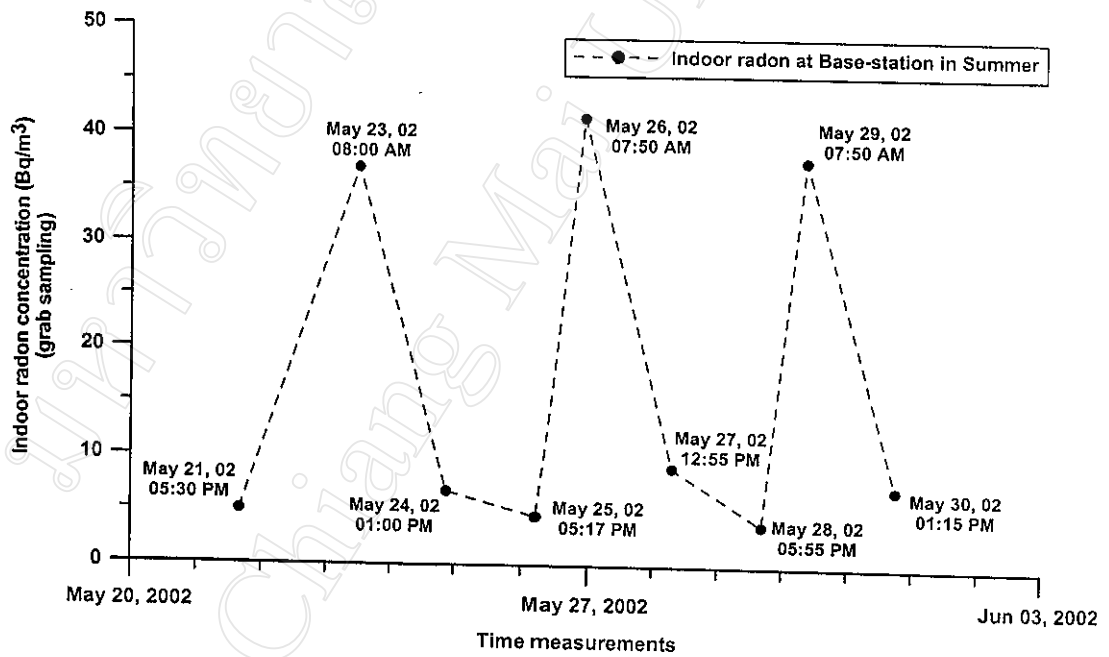


Figure 3.8 Summer indoor radon concentration in the base house.



The concentration of soil-gas radon was determined by injecting air drawn using a needle probe from soil exposed in a borehole and then sampling this air with the Scintrex radon meter.

Boreholes were drilled with a 37.5-millimeter hand auger. Figure 3.9 shows the operation sequences used to position the needle probe at the bottom of each borehole. Bentonite mixed with water to form a jelly, was placed at the bottom of a borehole (Figure 3.9a) and a PVC casing tube that was closed with plastic tape at the front end was pressed into the borehole. This caused the bentonite jelly to flow upwards between the casing and the soil, thus sealing the casing in the hole. This prevented gas from flowing up on the outside of the casing (Figure 3.9b). A 25-millimeter hand auger was then used to drill 20 centimeters below the casing (Figure 3.9c). A needle probe was then lowered down the casing and its end was positioned in the smaller hole. Finally, a rubber stopper was placed at the top of the casing to seal the needle probe in the borehole (Figure 3.9d). This procedure was designed to give maximum protection to the end of the probe and to minimize the disturbance to the soil in close vicinity to the point of measurement (Damkjaer and Korbech, 1992).

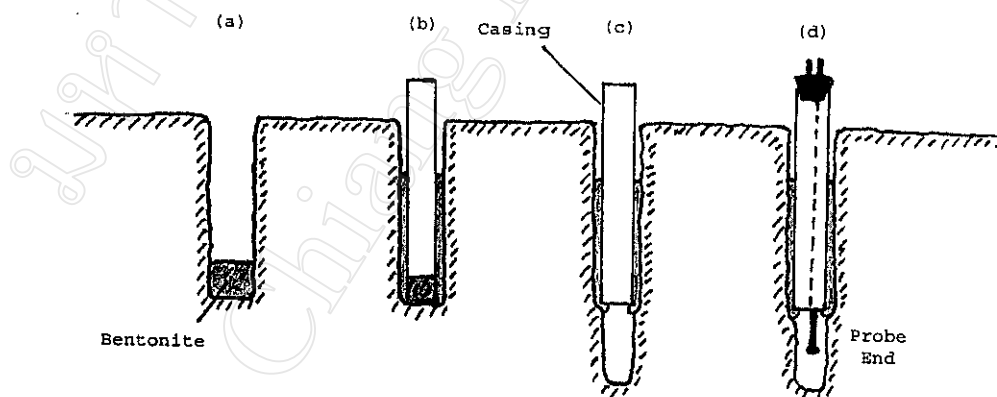


Figure 3.9 Sequence of operations used to position the needle probe in a borehole.

After a needle probe was placed in a borehole, a fresh cell was placed into the counters and the systems were allowed to adapt to the dark for 2 to 3 minutes. This ensured that no accidental light exposure contributed to the counting. Correct background data were obtained by counting the background for 1 minute before extracting soil-gas into the scintillation cell in the chamber. Soil-gas radon from the borehole was extracted six times, using a bulb pump to transfer the extracted soil-gas radon to the scintillation cell. Counting was done three times, for 1 minute each time. Figure 3.10 is a schematic diagram of the soil-gas radon extraction system.

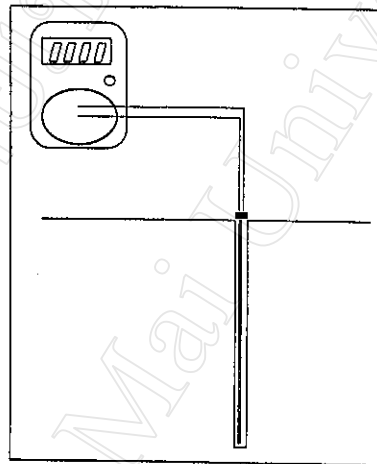


Figure 3.10 Schematic diagram of the soil-gas radon extraction system.

Soil-gas radon concentrations were measured from two depths, 0.5 and 1.0 meter, from two opposite corners of each of the 40 houses during three seasons. Measurements started in the rainy season, 11 September to 15 October 2001. However, in soil that was flooded as a result of the rainy season, no data concerning soil-gas radon concentrations and relative soil-gas radon permeability could be obtained. Additional measurements were made in winter from 28 January to 28 February 2002. The last measurements were made in summer from 21 May to 30 May 2002. The positions of the boreholes around a house are shown in Figure 3.11.

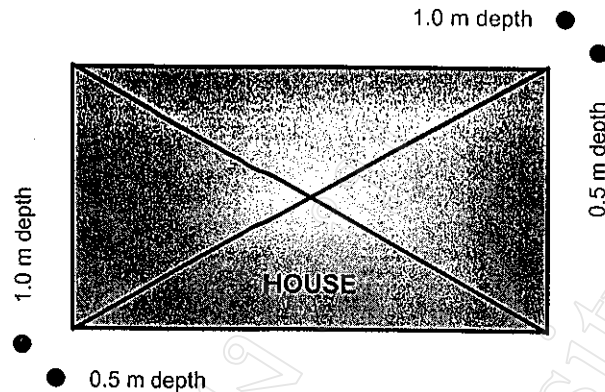


Figure 3.11 Boreholes positions

Soil-gas radon and thoron concentrations were determined using the following formula (Radical Calculation Software, 1994):

$$\text{Radon} = 0.87C_3 + 0.32C_2 - 0.34C_1 \quad (3.1)$$

$$\text{Thoron} = \frac{(C_1 + C_2 + C_3)}{3} - \text{Radon} \quad (3.2)$$

where,

- $C_1$  = 1st Minute Raw CPM – Cell Background
- $C_2$  = 2nd Minute Raw CPM – Cell Background
- $C_3$  = 3rd Minute Raw CPM – Cell Background

Soil-gas radon data in counts per minute were converted to soil-gas radon concentrations in  $\text{pCi.L}^{-1}$  and/or  $\text{Bq.m}^{-3}$  using a conversion factor calculated from the efficiency value of each scintillation cell. Each scintillation cell had been calibrated at the Office of Atomic Energy for Peace in Bangkok (appendix B). After being converted, two values of soil-gas concentration from each of the two depths from both corners of a house were averaged to get values for each house.

Figures 3.12 and 3.13 show the short-term variation of soil-gas radon concentration at the base house in the winter, 28 January to 28 February 2002, and summer seasons, 21 May to 30 May 2002, respectively. Figures 3.14 and 3.15 show the soil-gas radon concentrations results for the 40 houses.

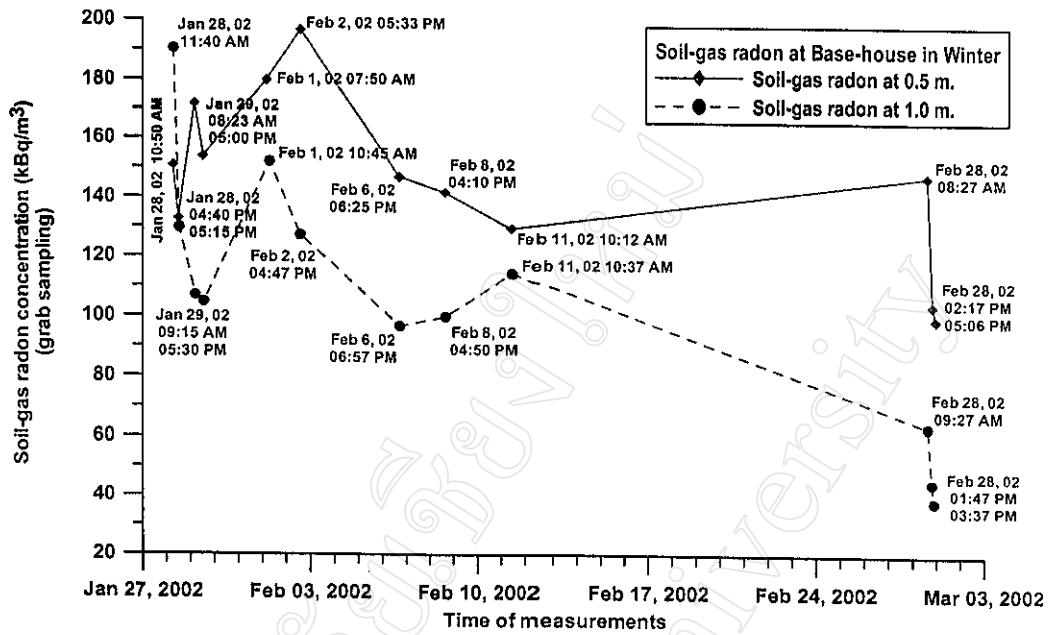


Figure 3.12 Grab sample soil-gas radon concentrations at the base house in the winter season

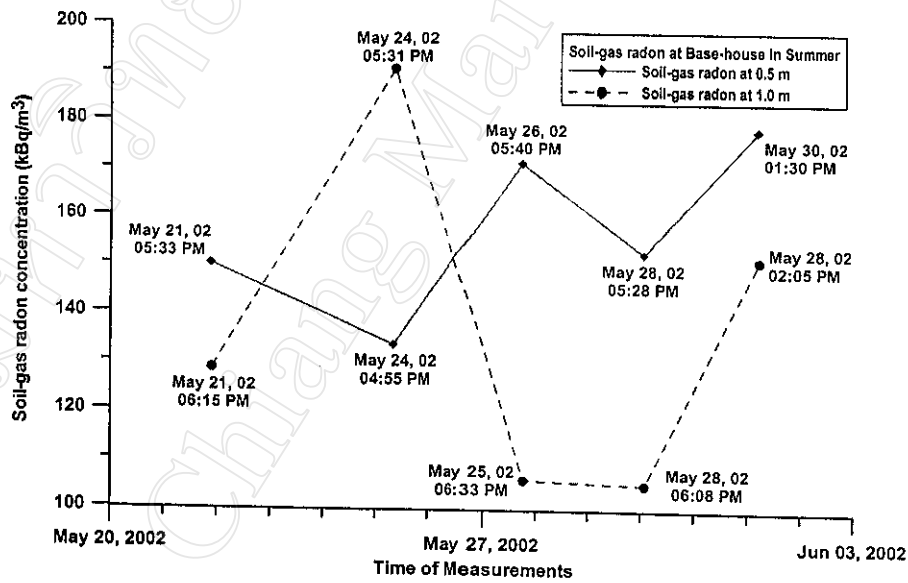


Figure 3.13 Grab sample soil-gas radon concentrations at base house in the summer season

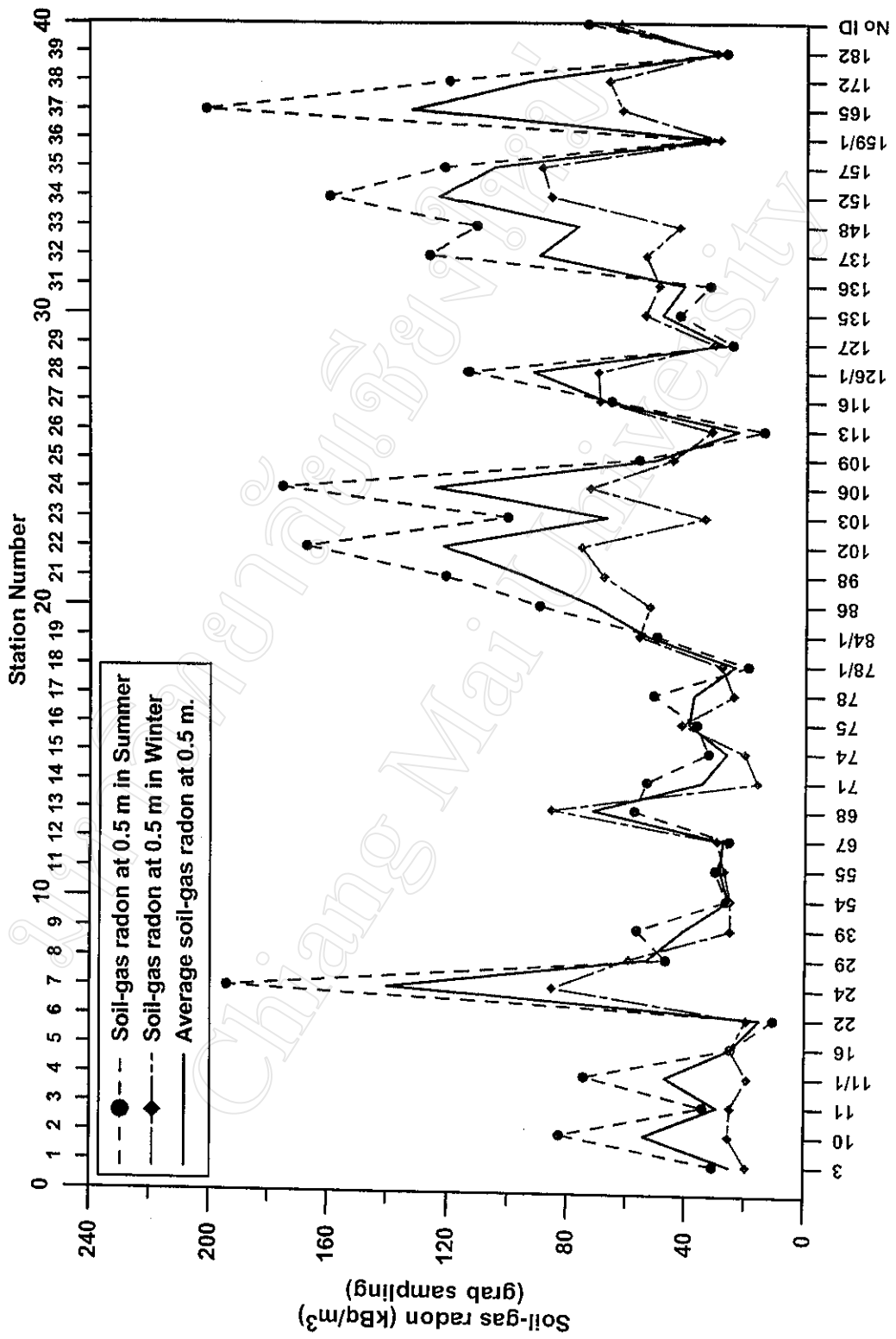


Figure 3.14 Grab sample soil-gas radon concentrations at 0.5-meter depth.

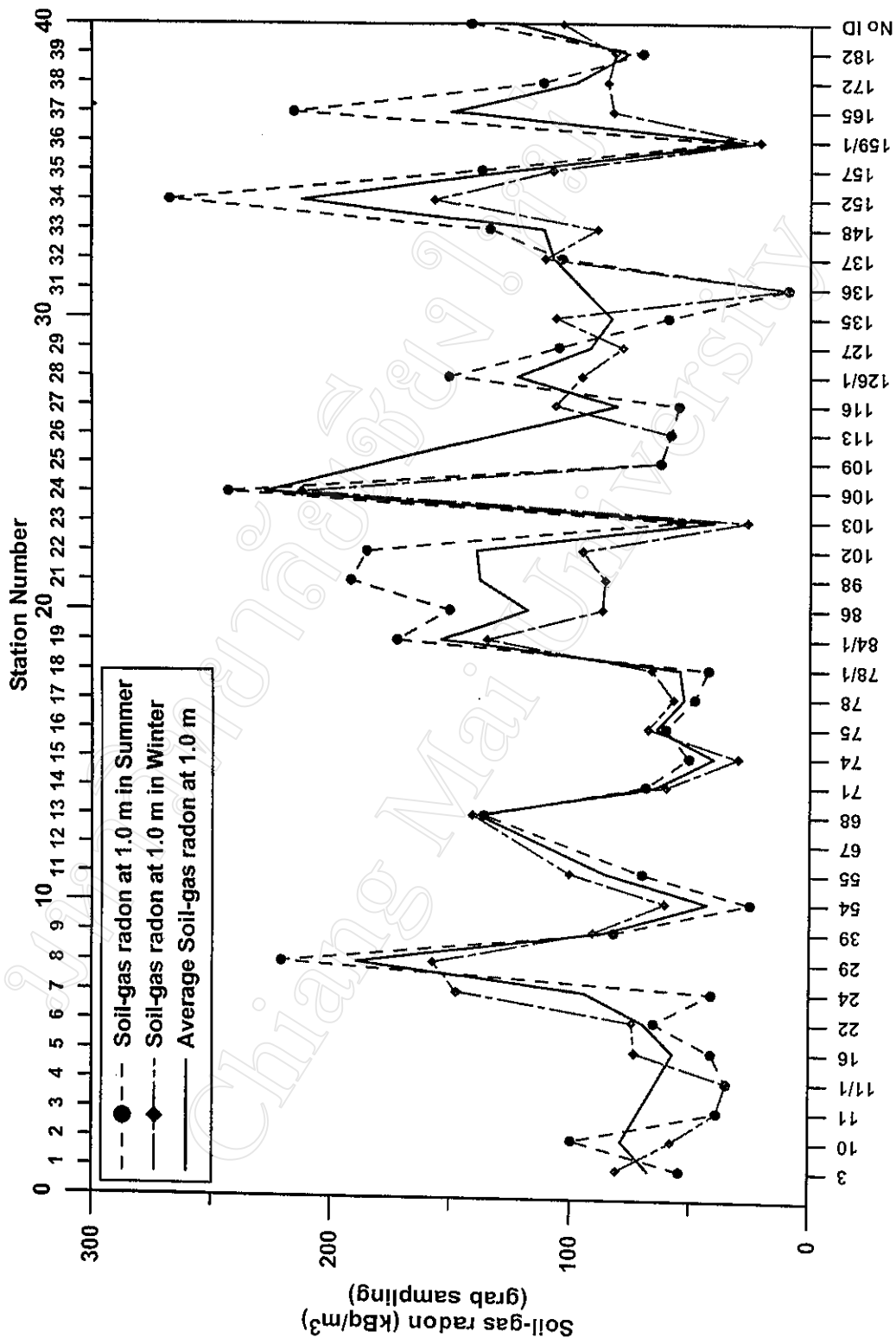


Figure 3.15 Grab sample soil-gas radon concentrations at 1.0-meter depth.

### 3.3 Relative soil-gas permeability measuring method

After soil-gas radon was measured and the needle probe was withdrawn, a perforated probe was inserted down the casing in each borehole. The head, or end, of this probe was below the casing and the passage between the casing and the probe shaft was closed at the surface with a rubber stopper.

Equation (2.8) can be rewritten as

$$k = \frac{\mu Q}{S \Delta p} \quad (3.3)$$

Figure 3.16 shows schematically the perforated probe below the surface. Since a cylindrical probe of length  $L$  and radius  $r$  is placed vertically at depth  $h$  beneath the surface, equation (3.3) can be rewritten as

$$k = \frac{\mu Q}{2\pi L \Delta p} \ln \left[ \frac{L}{r} \sqrt{\frac{4h-L}{4h+L}} \right] \quad (3.4)$$

where  $L \gg r$ .

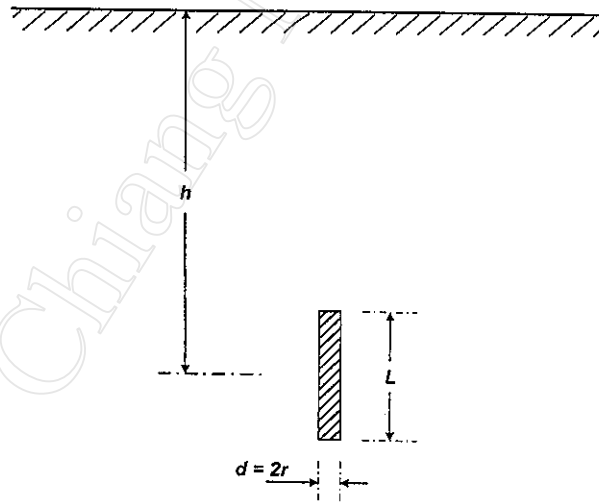


Figure 3.16 Schematic positioning of a perforated cylindrical probe buried in soil.

After the perforated probe was buried in soil, soil-gas permeability measurements were made. Figure 3.17 shows the arrangement of the pump used to make soil-gas permeability measurements and its connection to the perforated probe in the ground.

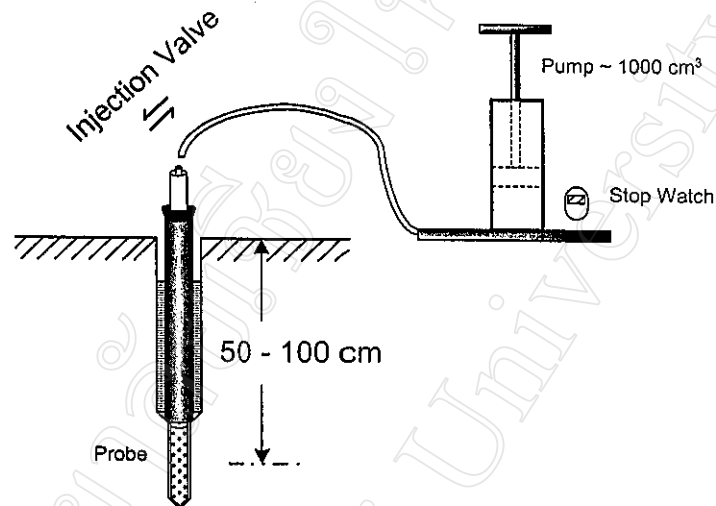


Figure 3.17 Arrangement of pump and its connection to the perforated probe for making relative soil-gas permeability measurements

The parameters for relative soil-gas permeability calculation at 0.5-meter depth are

$$\mu = 1.868 \times 10^{-5} \text{ Pa.s at } 25 \text{ }^\circ\text{C}$$

$$Q = \text{Volumetric flow rate (m}^3 \cdot \text{s}^{-1}\text{)}$$

$$= V_{pump} / (T_1 - T_0) ; V_{pump} = \text{pump volume}$$

$$= 1.032 \times 10^{-3} \text{ m}^3$$

$$T_1 = \text{time need to pump } V_{pump} \text{ at pressure } p \text{ into the soil}$$

$$T_0 = \text{time need to pump } V_{pump} \text{ at pressure } p \text{ in the free air}$$

$$\Delta p = \text{constant pressure } 3.834 \text{ kPa}$$

$$L = \text{perforated probe length } 0.199 \text{ m}$$

$$r = \text{radius of perforated probe } 0.0127 \text{ m}$$



Equation (3.4) can be rewritten as

$$k = 1.0665 \times 10^{-11} / (T_1 - T_0) \quad (3.5)$$

At a depth of 1.0 meter, the parameters for equation (3.4) are the same as the parameters for the relative soil-gas permeability calculation at a depth of 0.5 meter. With a difference of only the depth value, a change from 0.5 to 1.0 meter, equation (3.4) can be rewritten as

$$k = 1.08653 \times 10^{-11} / (T_1 - T_0) \quad (3.6)$$

The calculated relative soil-gas permeability values at a depth of 0.5 meter from the two sides of each house were averaged to obtain just one value. However, the average soil-gas permeability for a depth of 1.0 meter was obtained using values from both the 0.5 and 1.0 meter depths. This is because when radon migrates to the surface, it passes through the entire overlying soil column.

Figures 3.18 and 3.19 show the soil-gas permeability of 40 houses at depths of 0.5 meter and 1.0 meter, respectively.

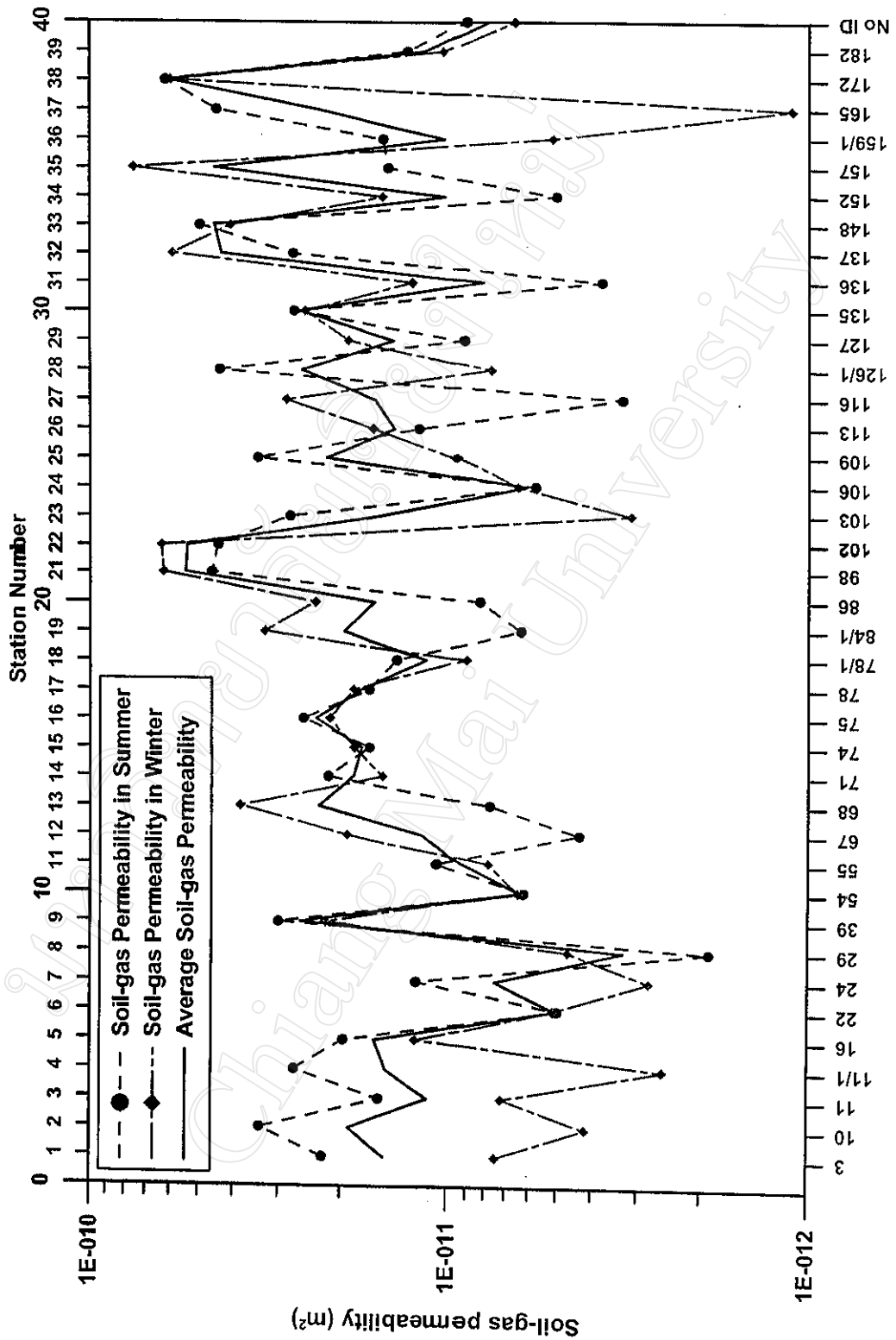


Figure 3.18 Soil-gas permeability of 40 houses at 0.5-meter depth in winter and summer

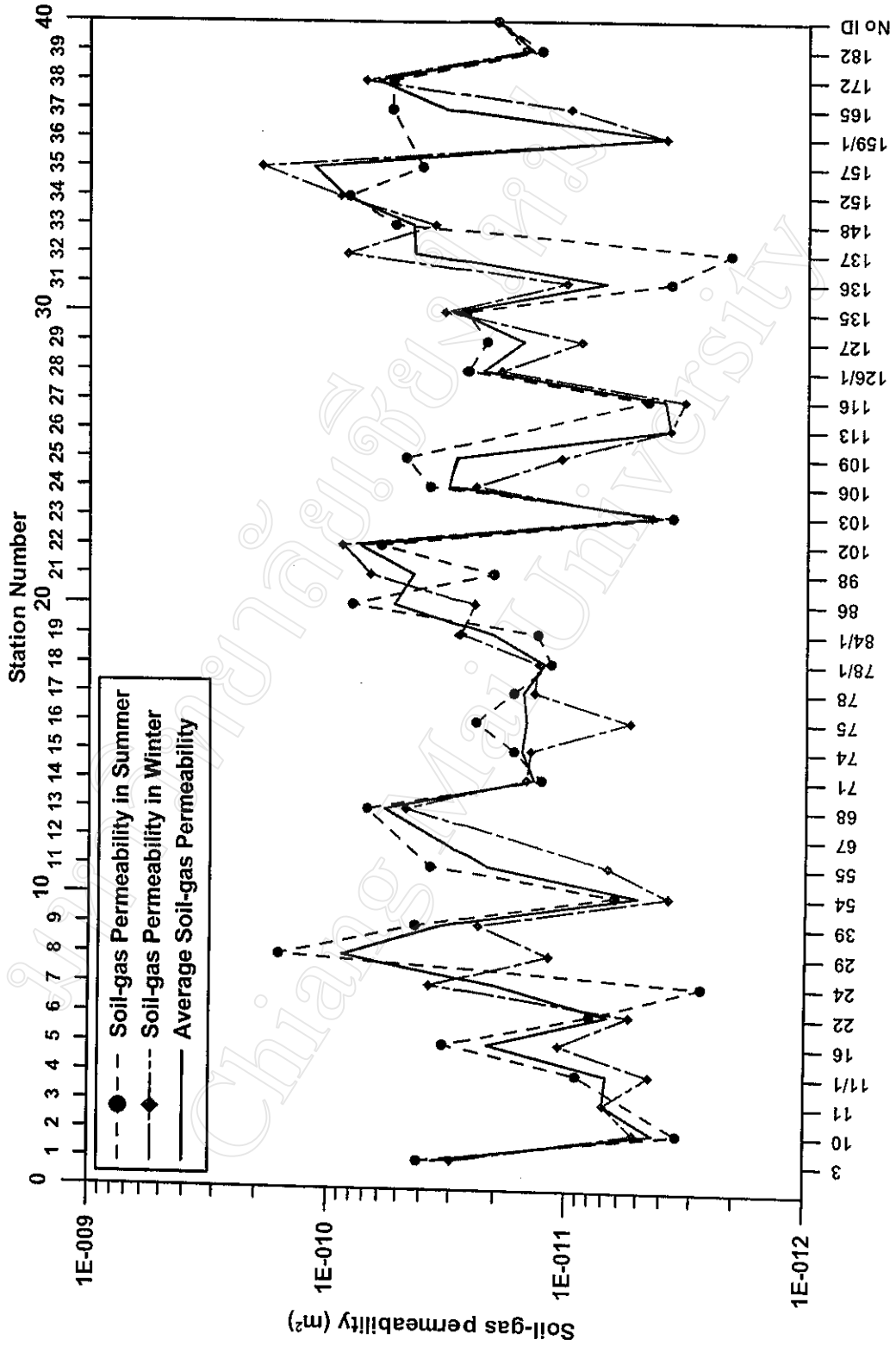


Figure 3.19 Soil-gas permeability of 40 houses at 1.0-meter depth in winter and summer